

## Experimental comparison of the phase-breaking lengths in weak localization and universal conductance fluctuations

D. Hoadley,\* Paul McConville,† and Norman O. Birge

*Department of Physics and Astronomy and Center for Fundamental Materials Research, Michigan State University, East Lansing, Michigan 48824-1116*

(Received 19 April 1999)

The observation of quantum transport phenomena in metals is limited by the eventual loss of phase coherence of the conduction electrons on the length scale  $L_\phi$ . We address the question of whether  $L_\phi$  is the same in the context of different quantum transport phenomena. Specifically, we have measured  $L_\phi$  from two different experiments on the same sample. The experiments are magnetoresistance and  $1/f$  noise versus magnetic field, and the samples are thin-Ag films in the quasi-two-dimensional regime. We determine  $L_\phi$  from fits of the magnetoresistance data to weak-localization theory (WL), and from fits of the noise versus magnetic field to universal conductance fluctuation theory (UCF). We find that the two values of  $L_\phi$  are the same at temperatures above about 10 K, but that  $L_\phi$  in the UCF experiment is shorter than that in the WL experiment at lower temperatures. This result is consistent with a recent theoretical discussion of quasielastic electron-electron scattering in disordered metals. [S0163-1829(99)00132-0]

### I. INTRODUCTION

A key ingredient in quantum transport phenomena in disordered solids is the phase coherence of conduction electrons over distances much longer than the elastic mean-free path. Although quantum phase coherence is crucial for localization of electronic wave functions,<sup>1-3</sup> discussion of the phase-coherence length didn't appear in the literature until 1979 in the context of weak-localization theory.<sup>4-9</sup> The beauty of quantum phase coherence in disordered solids only became widely appreciated a few years later with the experimental observation of the Aharonov-Bohm effect in disordered metal cylinders<sup>10</sup> and small rings,<sup>11,12</sup> and the discovery of universal conductance fluctuations (UCF) in small wires.<sup>13-16</sup> These experiments demonstrated convincingly that elastic scattering from nonmagnetic, static impurities does not destroy phase coherence of conduction electrons.

With the arrival of weak-localization theory, theorists started calculating the rates of inelastic scattering processes that destroy phase coherence.<sup>17-20</sup> In nonmagnetic systems, phase breaking is due mainly to inelastic electron-phonon and electron-electron scattering, which occur at much higher rates in disordered solids than in crystalline solids.<sup>21</sup> Much attention was paid in the 80s to the dephasing rate due to electron-electron scattering, because this is the dominant dephasing process in nonmagnetic samples at temperatures below a few K. Altshuler, Aronov and Khmelnitskii<sup>17</sup> showed that the electron-electron scattering rate in low-dimensional samples is dominated by collisions with small energy transfer, the so-called Nyquist scattering rate. Several groups performed experiments to measure the temperature dependence of the phase-breaking rate in one-dimensional (1D)<sup>22,23</sup> and (2D) systems.<sup>24</sup>

Despite the wealth of theoretical and experimental work on dephasing performed in the 80s, some questions remain today. A natural question that arises is whether the phase-breaking rate  $\tau_\phi^{-1}$  and hence the phase-breaking length  $L_\phi$

$=\sqrt{D\tau_\phi}$ , is expected to be the same for different quantum transport phenomena. ( $D=\frac{1}{3}v_F l_e$  is the electron diffusion constant, where  $v_F$  is the Fermi velocity and  $l_e$  is the elastic mean-free path.) Surprisingly, this question was not addressed in the 80s, perhaps because most of the theoretical calculations of  $\tau_\phi^{-1}$  were performed before the discovery of UCF. In 1990, Stern, Aharonov and Imry<sup>25</sup> showed theoretically that the dephasing rates for  $h/e$  and  $h/2e$  Aharonov-Bohm oscillations could be different in the case of dephasing by magnetic impurities. (Those two types of oscillations are directly related to UCF and weak-localization (WL) physics, respectively.) Those authors also discussed the Nyquist dephasing rate in their paper, but did not discuss the issue of whether the Nyquist rate might be different in the context of WL and UCF. Chandrasekhar, Santhanam, and Prober<sup>26</sup> also mentioned the possibility that the dephasing lengths for UCF and WL might be different, but they did not present any experimental evidence indicating which one is larger. This question was first addressed experimentally by us in 1993, when we determined  $L_\phi$  from two different measurements on a quasi-2D Ag film.<sup>27</sup> Fits of WL theory to magnetoresistance data yield a value we call  $L_\phi^{\text{WL}}$ , while fits of UCF theory to  $1/f$  noise versus magnetic-field data yield a value  $L_\phi^{\text{UCF}}$ . We found that the two values agreed at temperatures of 10 and 25 K, but that  $L_\phi^{\text{UCF}}$  was somewhat shorter than  $L_\phi^{\text{WL}}$  at temperatures of 1 and 4 K. The primary limitation of that work was that only one sample was measured, and only at four temperatures.

We present here a more complete set of measurements of the sort we reported earlier,<sup>27</sup> along with a full discussion of the theory. We have measured two new quasi-2D Ag samples at 10 temperatures between 1 and 30 K. Our new results confirm our earlier results, and show clearly that  $L_\phi^{\text{UCF}} \approx L_\phi^{\text{WL}}$  above 10 K, but  $L_\phi^{\text{UCF}} < L_\phi^{\text{WL}}$  below 10 K. In the meantime, Blanter<sup>28</sup> has published a theoretical paper where he claims that  $L_\phi^{\text{UCF}}$  and  $L_\phi^{\text{WL}}$  should be different in 1D or 2D at low temperature. While  $L_\phi^{\text{WL}}$  is indeed determined by the

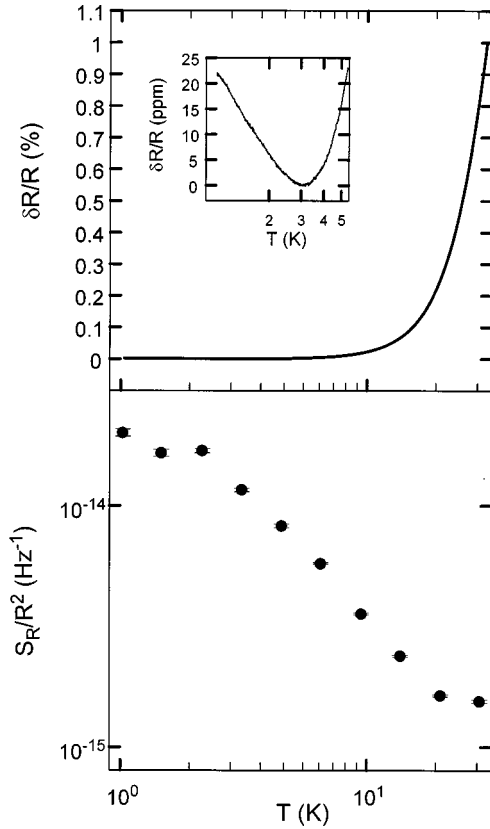


FIG. 1. (a) Resistance versus temperature; and (b) normalized  $1/f$  resistance noise power, evaluated at 1 Hz, versus temperature. Both figures show data from Ag sample 1, which has lateral dimensions  $7 \mu\text{m} \times 107 \mu\text{m}$  and is 14-nm thick. Inset: Expanded view of the low-temperature resistance versus temperature, showing the effects of weak localization and electron-electron interactions.

Nyquist dephasing rate, Blanter finds that  $L_\phi^{\text{UCF}}$  is determined by a different rate, called the out-scattering rate, which coincides in 2D with an alternative calculation of the dephasing rate presented in the 80s.<sup>19-20</sup> More to the point, Blanter finds theoretically that  $L_\phi^{\text{UCF}} < L_\phi^{\text{WL}}$  at low temperature, in agreement with our experiment. We find that the absolute values of the dephasing rates are in good agreement with Blanter's predictions, with no adjustable fitting parameters.

The issue of dephasing has attracted renewed interest recently due to the observation that the dephasing rate in some samples saturates at finite temperature,<sup>29</sup> in disagreement with the theoretical prediction. We note here that the interpretation of the results in Ref. 29 is highly controversial.<sup>30</sup> Unfortunately, the measurements reported in this paper are restricted to temperatures above 1 K, so we can not address the issue of  $L_\phi$  saturation here.

## II. EXPERIMENT

Two 14 nm-thick polycrystalline silver films were deposited onto high-resistivity silicon substrates cooled to 130 K under a pressure of  $10^{-7}$  torr. The samples were patterned into 5-terminal devices using standard optical lithography and lift-off processing. Lateral dimensions were  $7 \mu\text{m} \times 107 \mu\text{m}$  (sample 1) and  $18 \mu\text{m} \times 330 \mu\text{m}$  (sample 2). In order to maintain the grain sizes at about 10 nm and avoid

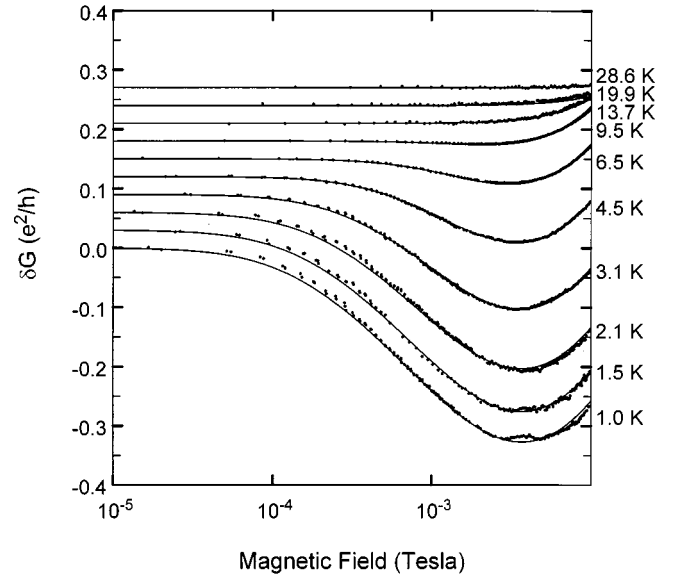


FIG. 2. Magnetoconductance of Ag sample 1 at 10 temperatures between 1.0 and 28.6 K. The solid lines are fits to weak localization theory [Eq. (1) in the text] with the fixed value of  $L_{so} = 0.44 \mu\text{m}$  obtained from the five lowest temperature fits. Values of  $L_\phi$  obtained from the fits are shown in Fig. 5.

excessive annealing at room temperature, the samples were quickly mounted in the cryostat and cooled to 77 K within 12 h. The sheet resistances of the samples at low temperature were  $4.8 \Omega$  and  $3.8 \Omega$  for samples 1 and 2, respectively. Resistance and noise measurements were made on the samples in the temperature range from 1 to 28.6 K in a pumped liquid  $\text{He}^4$  cryostat. The temperature dependence of the resistance is shown in Fig. 1(a). Below 10 K, the resistance increases with decreasing temperature due to weak localization and electron-electron interaction effects

Magnetoconductance measurements were made in a 4-terminal configuration with a lock-in amplifier. A ratio transformer was used to increase the sensitivity of the measurement to small changes in resistance. Noise measurements were made using a 5-terminal ac bridge technique.<sup>31</sup> Power spectra were taken with several bandwidths, the choice of which was based on the signal-to-noise ratio at a given temperature. These ranged from 0.05–1.25 Hz to 0.5–12.5 Hz. (The  $1/f$  frequency dependence of the noise power was constant over this frequency range.) The first stage of amplification in both measurements was a liquid-nitrogen-cooled Triad G-5 transformer. We tested for Joule heating at each measurement temperature using low-field magnetoconductance data taken at several excitation currents. The drive level for the noise measurements (and for the magnetoconductance data shown) was chosen such that its effect on the value of  $L_\phi$  inferred from the magnetoconductance fits was no more than a few percent.

## III. MAGNETORESISTANCE AND WEAK LOCALIZATION

Magnetoconductance data on sample 1 are shown in Fig. 2, for temperatures between 1.0 and 28.6 K. At low temperatures, the conductance first decreases then increases with in-

creasing magnetic field. This is the characteristic signature of a sample with moderate spin-orbit scattering. Normal weak localization is due to the constructive interference of time-reversed paths that return to the origin. Spin-orbit scattering rotates the relative spin directions of the two paths, causing destructive interference and weak ‘‘antilocalization’’ for paths with lengths  $L$  such that  $L_{so} < L < L_\phi$ , where  $L_{so} = \sqrt{D}\tau_{so}$  is the spin-orbit scattering length. At low-magnetic fields, the antilocalization is suppressed starting at the field scale corresponding to the dephasing length,  $B_\phi \approx (h/e)/L_\phi^2$ . When the field surpasses the spin-orbit field scale,  $B_{so} \approx (h/e)/L_{so}^2$ , the sign of the magnetoresistance changes as the localizing effect of paths with  $L < L_{so}$  is suppressed.

The theory of weak localization gives the magnetoconductance in the 2D limit as the following combination of digamma functions:<sup>7,9</sup>

$$\sigma(\omega=0, B) = -\frac{e^2}{2\pi^2\hbar} \left[ \Psi\left(\frac{1}{2} + \frac{B_1}{B}\right) + \frac{1}{2}\Psi\left(\frac{1}{2} + \frac{B_2}{B}\right) - \frac{3}{2}\Psi\left(\frac{1}{2} + \frac{B_3}{B}\right) \right], \quad (1)$$

where  $B_1 = B_0 + B_{so}$ ,  $B_2 = B_\phi$ , and  $B_3 = (4/3)B_{so} + B_\phi$ , and the characteristic fields are defined by  $B_0\tau_0 = 3\hbar/(4eD)$ , and for  $B_\phi$  and  $B_{so}$ :  $B_x\tau_x = \hbar/(4eD)$ . Here,  $\tau_0$  is the mean time between elastic scattering events. The expressions for  $B_1$  and  $B_3$  are valid when there is no appreciable magnetic impurity (spin-flip) scattering, which we believe to be the case for these samples.<sup>32</sup>

Fits of Eq. (1) to the data are shown in Fig. 2. There were two parameters involved in these fits, namely  $B_\phi$  and  $B_{so}$ . Evaluation of  $B_{so}$  is robust only at low temperature where the samples are in the strong spin-orbit scattering regime, i.e.,  $L_{so} < L_\phi$ . The values obtained at 1, 1.5, 2.1, 3.1, and 4.5 K were averaged and the entire data set fit to one value of  $B_{so}$ , since spin-orbit scattering is expected to be temperature independent.<sup>9</sup> The fit gave a value of  $L_{so} = 0.44 \mu\text{m}$ .  $L_\phi$  at each temperature is obtained from the fits with this fixed value of  $L_{so}$ .

We note that at the lowest temperatures measured, there is reason to doubt the validity of Eq. (1).<sup>33,34</sup> A discussion of this issue will be postponed to Sec. V, after we have discussed the noise measurements and the temperature dependence of  $L_\phi$ .

#### IV. $1/f$ NOISE AND UNIVERSAL CONDUCTANCE FLUCTUATIONS

Resistance noise in disordered metals arises from the motion of atomic defects.<sup>35</sup> When the relaxation times of the defects are very broadly distributed, the noise obeys a power-law frequency dependence, and is called  $1/f$  noise. Such a broad distribution occurs for thermally activated processes when the distribution of barrier heights is broad compared to  $k_B T$ .<sup>36</sup> At low temperature, defects move by quantum-mechanical tunneling, and the broad distribution of relaxation times arises from the exponential dependence of the tunneling rate on particle mass, barrier height, tunneling distance, etc. Low-temperature  $1/f$  noise has been observed in

several different materials.<sup>27,37–40</sup>

As the temperature is lowered and  $L_\phi$  becomes longer than  $l_e$ , the sensitivity of the sample’s conductance to its microscopic impurity potential increases. Sample-to-sample fluctuations in the conductance approach the universal value of  $e^2/h$  in a phase-coherence volume, and are called universal conductance fluctuations, or UCF. Experimentally, UCF are usually observed as static fluctuations as a function of applied magnetic field<sup>13</sup> or chemical potential<sup>14</sup> in a single mesoscopic sample at low temperature. But UCF can also be observed dynamically. In the UCF regime, the conductance of a phase-coherence volume can be sensitive to the motion of even one atomic-scale scatterer.<sup>41,42</sup> This extraordinary sensitivity leads to an enhancement of  $1/f$  noise relative to the classical (high-temperature) result.

Figure 1(b) shows the normalized resistance noise power of sample 1 at 0.2 Hz vs temperature.  $S_R$  is roughly proportional to  $1/T$  from 28.6 K down to about 6.5 K, and between 1 and 6 K it varies as  $T^{-1/2}$ . The observed increase of noise with reduced temperature is indicative of the UCF regime. In the simplest 2D case one can express the temperature dependence of the UCF noise power as  $S_R(T) \propto n_s(T)L_{th}^2 L_\phi^2$ , where  $n_s(T)$  is the density of mobile scatterers as a function of temperature and  $L_{th} = \sqrt{\hbar D/k_B T}$  is called the thermal length.<sup>37</sup> This description does not suffice here, however. As the ratio of  $L_\phi$  to  $L_{so}$  changes, we expect the amplitude of the UCF noise to change as well. In the limit of  $L_\phi \gg L_{so}$  (strong-spin-orbit scattering), the noise amplitude should be reduced by a factor of four relative to the weak-spin-orbit limit.<sup>43–46</sup> This crossover competes with the increasing  $L_\phi$  and  $L_{th}$  in the above expression to weaken the temperature dependence.

UCF-enhanced noise also features a strong magnetic-field dependence.<sup>37,43–45</sup> The effect can be explained either via random matrix theory by an analysis of the eigenvalue statistics of the sample Hamiltonian or transfer matrix, or from a Green’s-function calculation. In the latter approach, noise arises equally from the Cooperon and diffuson basis states in zero field. As the magnetic field is applied, the Cooperon contribution decreases over a field scale  $B_C = A(h/e)/L_\phi^2$  in a quasi-two-dimensional sample, where the constant  $A$  depends weakly on  $L_{th}$  and  $L_{so}$ . When  $B \gg B_C$ , the UCF noise is reduced by a factor of two. UCF theory gives a prescription to calculate the field dependence of the UCF-enhanced  $1/f$  noise.<sup>44</sup> The noise crossover function is defined as

$$\nu(B, T) \equiv \frac{S_G(B, T)}{S_G(0, T)}, \quad (2)$$

where  $S_G(B, T)$  is the conductance noise power at a chosen frequency as a function of magnetic field and temperature. (Since the conductance changes only very slightly with  $B$  in these experiments, the field dependence of conductance noise power and of resistance noise power are practically indistinguishable.) Measurement of the field dependence of the noise provides an excellent way to determine  $L_\phi$  in the context of UCF. The advantages of this noise reduction technique over the more typical magnetofingerprint measurement (static conductance fluctuations versus field) are twofold. In 2D, the characteristic field scale for the magnetofingerprint is related to  $L_{th}$ , while the field scale for the noise reduction is

related to  $L_\phi$ . A second consideration is experimental statistics. In a magnetofingerprint measurement, the range of magnetic field covered must be many times larger than the correlation magnetic field, so that one can extract an autocorrelation function averaged over many fluctuations. In the temperature range of our experiment it would require an inaccessibly large range of field to obtain proper statistics to satisfactorily determine  $L_\phi$ . For noise measurements, the range of magnetic field need only be of the same order as the correlation field. The noise power at fixed field already represents an average over contributions from all the mobile defects in the sample; the noise statistics can be improved simply by averaging over longer times.

The noise crossover function,  $\nu(B)$  in Eq. (2), has been calculated theoretically in the limits of  $L_{th}$  and  $L_{so}$  either much greater than or much less than  $L_\phi$ .<sup>44</sup> In our silver samples, these three lengths are comparable in the experimental temperature range. For example, at 4.5 K  $L_\phi \approx 0.7 \mu\text{m}$ ,  $L_{th} \approx 0.1 \mu\text{m}$ , and  $L_{so} \approx 0.5 \mu\text{m}$ . To obtain proper fits to our data, we have evaluated the theoretical functions numerically for arbitrary  $L_{th}$  and  $L_{so}$ . Spin-orbit scattering is accounted for by separating the singlet and triplet contributions in the Cooperon channel, following the work of Chandrasekar, Santhanam, and Prober.<sup>47</sup> Finite temperature introduces thermal smearing that is evaluated by numerical integration of Eq. (4) in Ref. 44. The details of the calculation are given in the appendix.

Figures 3(a), 3(b), and 3(c) show the normalized noise versus field data at ten temperatures. As the temperature is lowered, the magnetic-field scale characterizing the noise reduction decreases, indicating growth of  $L_\phi$ . In principle, we should fit these data to the noise crossover function  $\nu(B)$  given by Eq. (A9) in the Appendix, with the same two free parameters we used in the weak localization fits to the magnetoresistance, namely  $L_\phi$  and  $L_{so}$ . In practice, however, we found that the shape of  $\nu(B)$  depends only weakly on  $L_{so}$ , so it is difficult to obtain an accurate determination of  $L_{so}$  from the noise data alone. Hence, we used the value of  $L_{so}$  obtained from the magnetoresistance fits. No significant deviation from this value was detected by the fits to the data of noise vs magnetic field. A second consideration in fitting the data of Fig. 3 comes from the observation that at temperatures of 6.5 K and above the noise does not drop to  $\frac{1}{2}$  of its zero-field value, as expected from UCF theory. When  $L_\phi$  is not much greater than  $l_e$ , the amplitude of the noise is not well described by UCF theory. Resistance noise can arise from changes in orientation of single anisotropic defects or by changes in relative position of two neighboring defects. These processes takes place on a length scale typical of the spacing between neighboring defects  $l_e$  hence, the induced noise is called ‘‘local interference’’ noise.<sup>48</sup> The local interference processes do not vary with small magnetic fields. A crude way of accounting for the mixture of local interference and long-range interference (i.e., UCF) noise in our samples is to add an extra fitting parameter called the ‘‘fraction UCF’’, or  $f_{UCF}$ .<sup>49</sup> Hence, the actual function we fit to the data is

$$\frac{S_G(B,T)}{S_G(0,T)} = f_{UCF}\nu(B,T) + (1-f_{UCF}), \quad (3)$$

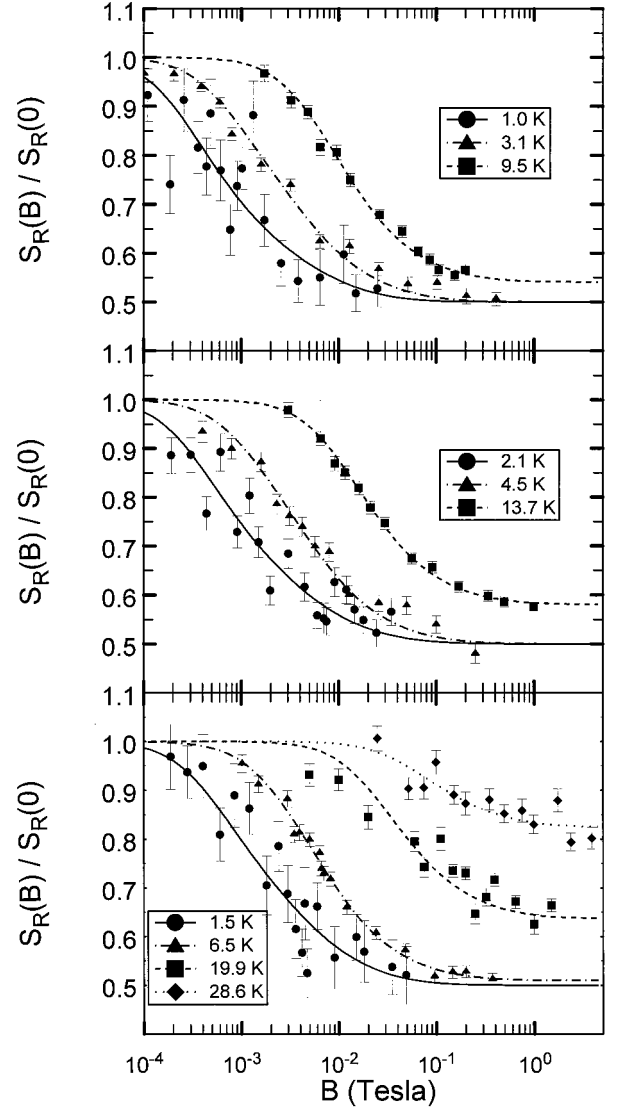


FIG. 3.  $1/f$ -noise power of Ag sample 1 versus magnetic field, normalized to its value at zero field, at 10 temperatures between 1.0 and 28.6 K. The lines are fits to universal conductance fluctuation theory [Eq. (3) in the text and Eq. (A9) in the Appendix] with the fixed value of  $L_{so} = 0.44 \mu\text{m}$ . Values of  $f_{UCF}$  and  $L_\phi$  obtained from the fits are shown in Figs. 4 and 5, respectively.

where  $\nu(B,T)$  is given by Eq. (A9) in the Appendix. This crude approach is justified by the excellent fits we obtain at the higher temperatures in Fig. 3. Figure 4 shows  $f_{UCF}$  versus temperature. As expected, this parameter is equal to 1 at low temperature, and starts to decrease rapidly above about 6 K.

## V. DISCUSSION

Figure 5, which is the central result of this work, shows  $L_\phi$  from the UCF and WL fits for all data taken on both samples. Above a few K,  $L_\phi$  exhibits strong temperature dependence, indicative of electron-phonon scattering. At lower temperatures the curves become less steep, indicative of a crossover to electron-electron scattering. The central issue of this paper is the comparison of the values of  $L_\phi$  from the two different experiments:  $L_\phi^{WL}$  and  $L_\phi^{UCF}$ . At our highest



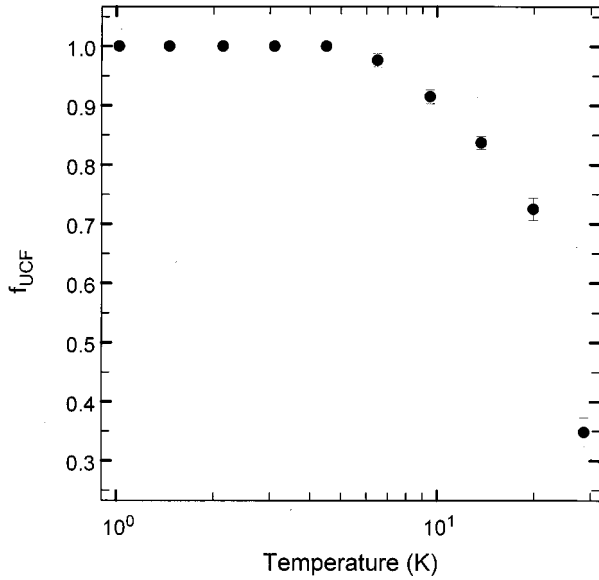


FIG. 4. Fraction UCF ( $f_{\text{UCF}}$ ) versus temperature, obtained from the fits shown in Fig. 3. At low temperature, the  $1/f$  noise is entirely attributed to UCF physics, whereas above about 6 K a magnetic-field-independent noise mechanism becomes increasingly important.

few measurement temperatures,  $L_{\phi}^{\text{WL}}$  and  $L_{\phi}^{\text{UCF}}$  agree. As we proceed to lower temperatures, however, we find increasing difference between the two. At 1 K, the ratio between the two values is about 1.6. The difference between  $L_{\phi}^{\text{WL}}$  and  $L_{\phi}^{\text{UCF}}$  cannot be dismissed as “within the noise,” because it is well outside of the statistical uncertainties shown in the figure. We believe that the difference is real, as we will show

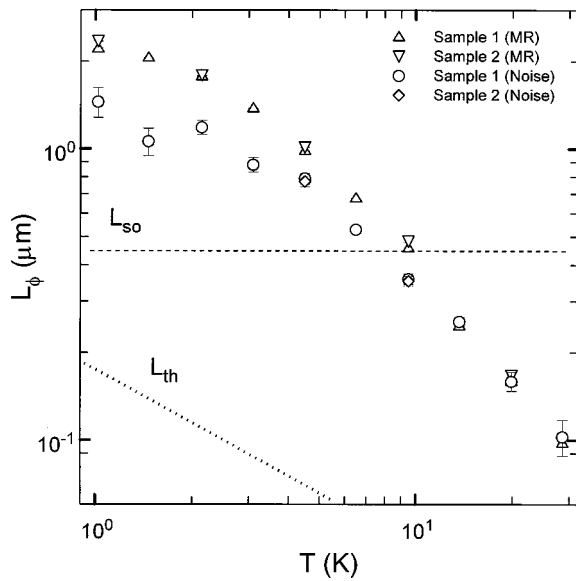


FIG. 5.  $L_{\phi}$  versus temperature for both Ag samples, obtained from the fits of weak-localization theory to the magnetoresistance data (Fig. 2) and the fits of UCF theory to the noise versus field data (Fig. 3). (Sample 2 was measured at every other temperature, and its noise was measured only at 4.5 K and above.) Above about 10 K, the values of  $L_{\phi}$  from the two different measurements are in agreement. At lower temperatures, the UCF value of  $L_{\phi}$  is consistently shorter than the WL value.

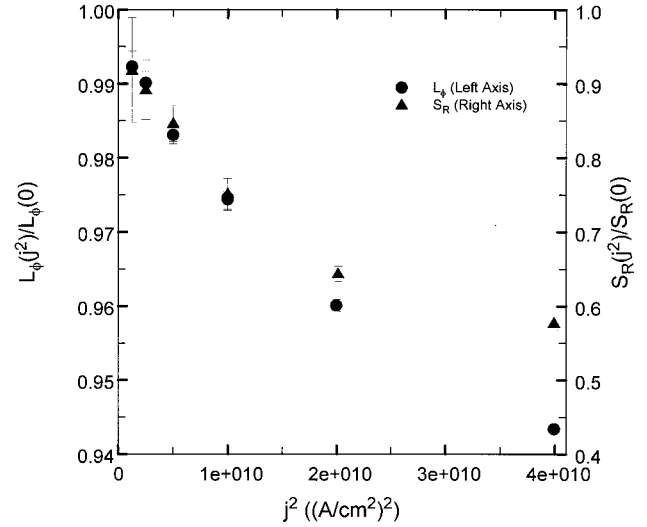


FIG. 6. Dependence on drive current of  $L_{\phi}$  (●), and noise power (▲), for sample 1 at 4.5 K. The noise decreases surprisingly quickly with increasing drive, whereas the value of  $L_{\phi}$  obtained from a fit of noise versus field is roughly 10 times less sensitive to drive.

below. But first we discuss several other ideas to rule out the possibility of systematic errors or experimental artifacts.

The first consideration is that sample 1, which is only  $7\text{-}\mu\text{m}$  wide, is approaching a dimensional crossover when  $L_{\phi}$  is of order  $1\text{ }\mu\text{m}$ . That is why we measured two samples with similar aspect ratios and very different widths. The figure shows that the value of  $L_{\phi}^{\text{UCF}}$  from sample 2 (width =  $18\text{ }\mu\text{m}$ ) agrees with that from sample 1 (width =  $7\text{ }\mu\text{m}$ ) at 4.5 K, and the values of  $L_{\phi}^{\text{WL}}$  agree at all temperatures. (Noise measurements were prohibitively time consuming on the larger sample below a few K.) Hence, we see no experimental evidence of dimensional crossover effects.

Uncertainty in our knowledge of the sample thickness will result in uncertainty in the calculated diffusion constant  $D$ . We used the Drude model and free-electron theory to obtain the mean-free path and diffusion constant from the resistivity. The values we found for sample 1 were  $l_e = 12\text{ nm}$  and  $D = 5.7 \times 10^{-3}\text{ m}^2/\text{s}$ , using the bulk value of the Fermi velocity of silver,  $v_F = 1.39 \times 10^6\text{ m/s}$ . The only sensitivity in the fitting process to  $D$  is through the thermal length, and the noise crossover function is quite insensitive to  $L_{\text{th}}$ . In fact, changing  $D$  by a factor of 3 introduces at most a 10% change in the value of  $L_{\phi}$  extracted from the fit at the lowest temperatures.

A further possible source of systematic error could have been sample heating due to the measurement current. As discussed earlier, we measured the magnetoresistance versus drive current at all temperatures to determine the maximum acceptable drive for the noise measurements. Our criterion was that  $L_{\phi}^{\text{WL}}$  was reduced by no more than a few percent from the extrapolated zero-drive value. Figure 6 shows  $L_{\phi}^{\text{WL}}$  versus current density squared for sample 1 at 4.5 K. At a current density of  $10^5\text{ A/cm}^2$ ,  $L_{\phi}^{\text{WL}}$  is reduced by only 2% from the extrapolated zero-drive value. To check whether this same drive level influenced  $L_{\phi}^{\text{UCF}}$ , we measured the noise versus field at that drive level and at half that level.

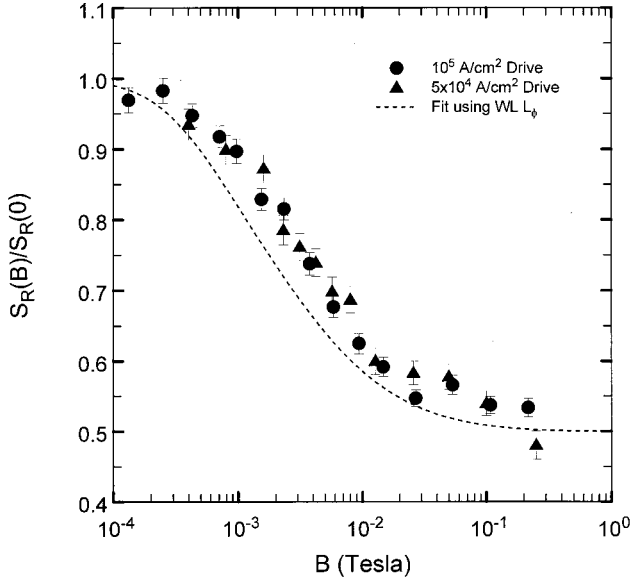


FIG. 7. Normalized noise versus magnetic field for sample 1 at 4.5 K, at two different drive currents. Not only are the data barely distinguishable, but both are clearly incompatible with the predicted dependence (dashed line) based on the WL value of  $L_\phi$  at this temperature.

The results are shown in Fig. 7. There is no noticeable shift between these data sets. Furthermore, the dotted line in Fig. 7 is the theoretical crossover function obtained by using the value of  $L_\phi$  from the magnetoresistance. This curve is clearly incompatible with the data, demonstrating that joule heating from the drive current cannot be the source of the observed difference between  $L_\phi^{\text{UCF}}$  and  $L_\phi^{\text{WL}}$ .

One aspect of the drive dependence of the noise is perplexing. The noise at fixed field is apparently far more sensitive to drive heating than its field dependence, or than the magnetoresistance. Figure 6 shows also the drive dependence of the zero-field noise of sample 1 at 4.5 K. At a drive of  $10^5$  A/cm<sup>2</sup>, the noise was reduced by 20% relative to the extrapolated zero-drive value, even though such a drive hardly affected the magnetoresistance or the field dependence of the noise. We tried to model this effect by heating. Using the measured temperature dependence of the zero-field noise and of  $L_\phi^{\text{UCF}}$ , and the known temperature dependence of  $L_{\text{th}}$ , we can infer the temperature dependence of the density of mobile defects,  $n_s(T)$ . [We assume for simplicity that the spin-orbit scattering crossover occurred at temperatures above 4.5 K. Eliminating this assumption does not improve the agreement between the heating model and the data.] To obtain the strongest dependence of noise on drive within a heating model, we assume that the defects are thermally linked to the phonons, while  $L_\phi^{\text{UCF}}$ , and  $L_{\text{th}}$  are determined by the temperature of the conduction electrons. Even with these best-case assumptions, the heating model is not capable of explaining the 10-fold difference between the noise and the  $L_\phi$  sensitivity to drive. Of course, the best thing to do would be to make all measurements with a drive current that does not noticeably affect either the magnetoresistance or noise measurements. At the lowest temperatures, however, that was impractical due to the signal-to-noise limitations of the noise measurement. In any case, we reiterate that the

values of  $L_\phi^{\text{UCF}}$  obtained from the fits of noise versus field are robust, as Fig. 7 shows.

Another consideration is the role of spin-flip scattering, which we have not included in our WL and UCF fits. According to the theories, spin-flip scattering enters into the dephasing rates differently for WL and UCF. For UCF, we have  $\tau_{\text{total}}^{-1} = \tau_\phi^{-1} + \frac{4}{3}j\tau_{\text{so}}^{-1} + \tau_{\text{sf}}^{-1}$ , where  $j=0$  or  $1$  for the singlet and triplet contributions, respectively. For WL, the corresponding result is slightly more complicated, because spin-flip scattering enters the singlet and triplet contributions differently. We are interested in the low-temperature regime, where  $\tau_{\text{so}}^{-1} > \tau_\phi^{-1}$ .  $L_\phi^{\text{WL}}$  is determined by the low-field magnetoresistance, which in this case is dominated by the singlet contribution to WL:  $\tau_{\text{total-singlet}}^{-1} = \tau_\phi^{-1} + 2\tau_{\text{sf}}^{-1}$ . These expressions indicate that spin-flip scattering is expected to cause a greater dephasing rate in WL than in UCF. Hence, this cannot account for the difference we observe.

We believe that the experimental difference between  $L_\phi^{\text{UCF}}$  and  $L_\phi^{\text{WL}}$  indicates a true difference between the dephasing rates relevant for WL and UCF phenomena. Blanter has recently shown<sup>28</sup> that in the limit where the dominant dephasing mechanism is electron-electron scattering with small energy transfer (also called “quasielastic” scattering or Nyquist scattering<sup>17,18</sup>), WL and UCF phenomena are governed by two different dephasing rates. The appropriate rate for WL, which Blanter calls  $\tau_\phi^{-1}$ , is the dephasing rate first calculated by Altshuler, Aronov, and Khmel'nitskii in 1982.<sup>17</sup> The appropriate rate for UCF differs by a logarithmic factor, and is called the “out-scattering” rate, or  $\gamma_{\text{out}}$ . Ironically, the out-scattering rate was initially believed by several authors<sup>19–20</sup> in the 1980s to be the relevant rate for WL, although this disagreement was later cleared up by Fukuyama.<sup>50</sup> Blanter explains that the calculation of the out-scattering rate in Refs. 19–20 omitted a class of important diagrams in the diffusion propagator. Coincidentally, these are the same diagrams that do not contribute to the UCF diffusion propagator, which explains why those calculations produce the correct result for the UCF dephasing rate.

In 2D, the formula for the dephasing rate due to quasi-elastic electron-electron scattering, or the Nyquist rate, is<sup>17,18</sup>

$$\frac{1}{\tau_\phi} \approx \frac{G_0}{G} \frac{k_B T}{\hbar} \ln\left(\frac{G}{2G_0}\right) = \frac{3\pi k_B T}{2\hbar k_F^2 l t} \ln\left(\frac{k_F^2 l t}{3\pi}\right), \quad (4)$$

where  $G$  is the sheet conductance of the sample,  $G_0 = e^2/h$  is the conductance quantum, and  $t$  is the sample thickness. [The prefactor inside the logarithm of Eq. (4) varies slightly between Refs. 17 and 18.] The 2D form for the out-scattering rate is given by<sup>19,20</sup>

$$\gamma_{\text{out}} = \frac{3\pi k_B T}{4\hbar k_F^2 l t} \ln\left[\frac{\hbar D \kappa^2}{k_B T} \left(\frac{k_F^2 l t}{3\pi}\right)^2\right], \quad (5)$$

where  $\kappa = 4\pi e^2 n(E_F) t$  is the screening length, and  $n(E_F)$  is the density of states at the Fermi level. Plugging in the parameters for sample 1, we find  $\tau_\phi^{-1} = 2.6 \times 10^8$  s<sup>-1</sup> and  $\gamma_{\text{out}} = 6.4 \times 10^8$  s<sup>-1</sup> at  $T = 1$  K. Given our diffusion constant  $D = 5.7 \times 10^{-3}$  m<sup>2</sup>/s, this gives  $L_\phi^{\text{WL}} = 4.7$   $\mu$ m and  $L_\phi^{\text{UCF}} = 3.0$   $\mu$ m at 1 K. The theoretical values of the phase-breaking lengths are almost exactly a factor of two greater

than the experimental values at 1 K shown in Fig. 5. Equivalently, the theoretical rates are a factor of four smaller than the experimental rates. What is striking, though, is that the ratio of the lengths (or the rates) agrees very well with experiment for the data below about 3 K, which is the temperature range where these theoretical expressions are valid. The ratio of the rates is about 2.5 both from experiment and from theory, i.e.,  $\gamma_{\text{out}}/\tau_{\phi}^{-1} = 2.5 \approx (L_{\phi}^{\text{WL}}/L_{\phi}^{\text{UCF}})^2$  for  $T$  between 1 and 3 K. At higher temperature, the dephasing rates determined from the experiment follow a steeper temperature dependence, and the two dephasing rates merge. Both of these features are expected when electron-phonon scattering becomes the dominant dephasing mechanism.

The identification of the low-temperature dephasing mechanism as quasielastic electron-electron scattering introduces a complication in the interpretation of magnetic-field-dependent phenomena. Collisions with small energy transfer do not destroy phase coherence immediately. The phase is randomized only after several collisions or after passage of a sufficiently long time.<sup>17,18</sup> Hence, the Nyquist scattering rate does not simply add to other dephasing rates such as that associated with the magnetic field,  $\omega_B = 4DeB/\hbar$ . In principle, then, the expression for the weak-localization magnetoresistance, Eq. (1), and possibly also the expression for the field-dependence of UCF, Eq. (A.9), should be modified at low temperatures. This problem has been addressed theoretically by Altshuler, Altshuler, and Aronov<sup>33</sup> and by Eiler,<sup>34</sup> and its importance in 1D has been emphasized by Echernach *et al.*<sup>51</sup> For our 2D samples, we can estimate the error in our determination of  $L_{\phi}^{\text{WL}}$  from Eq. (1) following Eiler.<sup>34</sup> He shows that the magnetic-field dependence of the Nyquist scattering rate causes the magnetoresistance curve to flatten relative to Eq. (1) evaluated with the field-independent rate  $\tau_{\phi}^{-1}$ . The flattened curve is nearly indistinguishable from a curve of the form of Eq. (1), but evaluated with a slightly increased dephasing rate

$$\bar{\tau}_{\phi}^{-1} \approx \tau_{\phi}^{-1} \left( 1 - \frac{2G_0}{3G} \frac{k_B T \tau_{\phi}^{-1}}{\hbar} \right)^{-1/2}. \quad (6)$$

For our Ag samples, the correction term is about 6%, which leads to a correction of only 3% to the experimental determination of  $L_{\phi}^{\text{WL}}$  from Eq. (1). Note that the magnetic-field dependence of the Nyquist rate tends to increase the apparent scattering rate, hence it tends to decrease the experimentally determined value of  $L_{\phi}^{\text{WL}}$  relative to the true value. Making this correction to the data in Fig. 5 would only increase the difference between the experimental values of  $L_{\phi}^{\text{WL}}$  and  $L_{\phi}^{\text{UCF}}$ . We have chosen not to make the small correction because there is no mention in the theoretical literature of whether a similar correction is needed for  $L_{\phi}^{\text{UCF}}$ .

Although the theoretical explanation outlined above is gratifying, it does not address all aspects of the data. The theoretical scattering rates given by Eqs. (4) and (5) are linear in  $T$ , so that we expect  $L_{\phi} \propto T^{-1/2}$  at low temperature. The data in Fig. 5, however, show a slight flattening off of  $L_{\phi}$  vs  $T$  in the same temperature range where the theory predicts the correct ratio between the WL and UCF results. As mentioned earlier, saturation of  $L_{\phi}$  at low temperature has been observed in some other samples.<sup>29</sup> Due to the difficulty of

the noise measurements, we could not extend the data presented here to low enough temperature to address the issue of saturation.

## VI. CONCLUSION

We have measured the phase-breaking lengths associated with weak localization (WL) and universal conductance fluctuations (UCF) in two 2D Ag samples. Analysis of the UCF data required calculation of the noise crossover function for arbitrary values of  $L_{\text{so}}$  and  $L_{\text{th}}$  (the spin-orbit scattering length and thermal length, respectively) relative to the phase-breaking length. We find that the two phase-breaking lengths are the same at temperatures above 10 K, but they differ at low temperature. Between 1 and 3 K, the UCF dephasing rate is a factor of 2.5 larger than the WL dephasing rate. These results are consistent with a recent theoretical treatment of dephasing due to electron-electron collisions with small energy transfer, or Nyquist dephasing. We also show that corrections to the theoretical WL expression due to the peculiar behavior of Nyquist scattering are very small for our low-resistance samples.

The difference between the dephasing rates associated with WL and UCF should be even larger in the 1D regime than in the 2D regime studied here.<sup>28</sup> Experiments similar to those performed here, but on 1D wires, would provide yet a stronger test of the theoretical predictions.

## ACKNOWLEDGMENTS

We are grateful to Y. Blanter for helpful discussions, to A. D. Stone and S. Xiong for assistance with the theory, and to M. E. Gershenson for pointing out an error in the original manuscript. This work was supported by National Science Foundation under Grant Nos. DMR-9023458 and DMR-9321850.

## APPENDIX

Here, we outline the calculation of the UCF noise crossover function in a 2D conductor for arbitrary temperature and spin-orbit scattering. We follow the procedure of Altshuler and Spivak,<sup>41</sup> calculating the variance of the conductance in the unsaturated case ( $\delta G^2 \ll e^2/h$ ). Stone<sup>44</sup> described this calculation in a 2D sample, but without the treatment of spin-orbit scattering. We treat spin-orbit scattering following the work of Chandrasekhar, Santhanam, and Prober.<sup>47</sup> In the presence of spin-orbit scattering, the phase-breaking length,  $L_{\phi}$ , is no longer simply equal to the inelastic scattering length,  $L_{\text{in}}$ . The  $j=1$  triplet states have  $L_{\phi} = [L_{\text{in}}^{-2} + (4/3)L_{\text{so}}^{-2}]^{-1/2}$ , while  $L_{\phi} = L_{\text{in}}$  for the  $j=0$  singlet state.

We begin by considering the  $1/f$  noise reduction function,  $\nu(B)$ , given in Eq. (2) in the text. This function varies from 1 to  $\frac{1}{2}$  asymptotically as  $B$  increases. To make the connection between  $\nu(B)$  and UCF theory, we must consider the noise within a specified bandwidth, due to a subset of mobile defects in the sample. If we assume that the dynamics of that ensemble of defects is unchanged by the magnetic field, then the field dependence of the noise is given by the expression for the ensemble average of conductance fluctuations due to a change in the microscopic impurity potential

$$\begin{aligned}
S_G(B, T) &\propto [\delta G'(B, T)]^2 \\
&= \langle [\delta G(B, T, V) - \delta G(B, T, V')]^2 \rangle \\
&= 2\{\text{Var}[G(B, T)] - \langle \delta G(B, T, V) \delta G(B, T, V') \rangle\},
\end{aligned} \tag{A1}$$

where  $\text{Var}[G] \equiv \langle (\delta G)^2 \rangle$  and  $V$  and  $V'$  are the impurity configurations before and after movement of an impurity.<sup>44</sup> The second term above can be expressed as  $\text{Var}[G(\gamma_\phi + \gamma')]$ , where  $\gamma_\phi = \tau_\phi^{-1}$  and  $\gamma' = 1/\tau_\phi[1 - \langle VV' \rangle / \langle V \rangle^2]$  in the limit that  $\gamma' \ll \gamma_\phi$ .<sup>41</sup> These expressions are valid in the unsaturated regime, where the total conductance fluctuation amplitude in a coherence volume is much less than  $e^2/h$ . In that limit we can write

$$\text{Var}[G(\gamma_\phi + \gamma')] \approx \text{Var}[G(\gamma_\phi)] + \gamma' \left. \frac{d(\text{Var}[G(\gamma)])}{d\gamma} \right|_{\gamma=\gamma_\phi}. \tag{A2}$$

Then

$$S_G(B) \propto -2\gamma' \frac{d[\text{Var}(G)]}{d\gamma_\phi}, \tag{A3}$$

so

$$\nu(B) = \frac{\frac{d}{d\gamma_\phi} \{ \langle [\delta G(B, T, \gamma_\phi)]^2 \rangle \}}{\frac{d}{d\gamma_\phi} \{ \langle [\delta G(B=0, T, \gamma_\phi)]^2 \rangle \}}. \tag{A4}$$

Now we need to find  $\text{Var}[G(B, T, \gamma_\phi)]$ . This quantity can be divided into two contributions, which in diagrammatic theory are called the Cooperon and diffuson channels. The two contributions are equal in zero field, and only the former is reduced in the presence of a field. (We are neglecting the Zeeman reduction of the diffuson, which occurs at very high field.<sup>38,43</sup>) According to Stone,<sup>44</sup>

$$\begin{aligned}
\langle (\delta G_{\text{Cooperon}})^2 \rangle &= \left( \frac{e^2}{h} \right)^2 \left( \frac{16}{\pi^4} \right) \\
&\times \int_{-\infty}^{\infty} \frac{d(\Delta E)}{2k_B T} K \left( \frac{\Delta E}{2k_B T} \right) F_c(\Delta E, B),
\end{aligned} \tag{A5}$$

where  $K(x) = x \coth(x) - 1/\sinh^2 x$  and  $F_c(\Delta E, B)$  is the energy correlation function for the Cooperon given by

$$\begin{aligned}
F_c(\Delta E, B) &= \sum_n \left[ \frac{1}{4|\lambda_{n,j=0}|^2} + \frac{1}{8} \text{Re} \left( \frac{1}{\lambda_{n,j=0}^2} \right) + \frac{3}{4|\lambda_{n,j=1}|^2} \right. \\
&\left. + \frac{3}{8} \text{Re} \left( \frac{1}{\lambda_{n,j=1}^2} \right) \right].
\end{aligned} \tag{A6}$$

The  $\lambda_{n,j}$  are the eigenvalues of the Cooperon diffusion equation,

$$\left[ D \left( -i\nabla - 2 \frac{e}{\hbar} \mathbf{A} \right)^2 + \frac{1}{\tau_\phi} + \frac{4}{3} j \frac{1}{\tau_{\text{so}}} - i \frac{\Delta E}{\hbar} \right] \Psi_{n,j} = \lambda_{n,j} \Psi_{n,j}. \tag{A7}$$

As mentioned before,  $j=1$  corresponds to the spin-triplet eigenstates, and  $j=0$  the singlet state. The eigenvalues of the Cooperon equation are given by

$$\lambda_{n,j} = 4 \frac{e}{\hbar} B D \left( n + \frac{1}{2} \right) + \frac{1}{\tau_{\text{in}}} + \frac{4}{3} j \frac{1}{\tau_{\text{so}}} - i \frac{\Delta E}{\hbar}, \tag{A8}$$

with degeneracy determined by the area of our 2D samples,  $2BL_x L_z (e/h)$ . After taking a derivative of  $F_c(B)$  with respect to  $(1/\tau_\phi)$  we can express  $S_c(B)$ , the contribution to the noise from the Cooperon channel, as

$$\begin{aligned}
S_c(B) &\propto \int_{-\infty}^{\infty} \left\{ \frac{d(\Delta E)}{2k_B T} K \left( \frac{\Delta E}{2k_B T} \right) \sum_{n=0}^{3(h/e)/8\pi^2 l_e^2 B} \frac{2BL_x L_z}{h/e} \right. \\
&\left. \times \left[ \frac{1}{4} f(a_{n,s}, b) + \frac{3}{4} f(a_{n,t}, b) \right] \right\},
\end{aligned} \tag{A9}$$

where

$$\begin{aligned}
f(a_{n,x}, b) &= \left[ \frac{a_{n,x}(-3a_{n,x}^2 + b^2)}{(a_{n,x}^2 + b^2)^3} \right] \\
a_{n,s} &= \frac{8BL_z^2(n + \frac{1}{2})}{\pi(h/e)} + \frac{L_z^2}{\pi^2 L_\phi^2} \\
a_{n,t} &= \frac{8BL_z^2(n + \frac{1}{2})}{\pi(h/e)} + \frac{L_z^2}{\pi^2 L_\phi^2} + \frac{4L_z^2}{3\pi^2 L_{\text{so}}^2} \\
b &= \frac{\Delta E L_z^2}{\pi^2 \hbar D} = \frac{\Delta E}{k_B T} \frac{L_z^2}{\pi^2 L_{\text{th}}^2}.
\end{aligned}$$

The upper limit on the sum in Eq. (A9) corresponds to when the cyclotron orbit of an electron is comparable to  $l_e$ . Electrons with shorter cyclotron orbits do not contribute to the conductance fluctuations in the diffusive regime.

Equation (A9) is the result we need to fit our data via Eq. (3) of this paper. In the limit of low-magnetic field, we convert the sum to an integral. Further details are given in the Appendix of Ref. 52.

\*Present address: V.I. Engineering, 37800 Hills Tech Drive, Farmington Hills, MI 48331.

†Present address: Xerox Corporation, 800 Phillips Road, 147-59B, Webster, NY 14580.

<sup>1</sup>P. W. Anderson, Phys. Rev. **109**, 1492 (1958).

<sup>2</sup>D. J. Thouless, Phys. Rev. Lett. **39**, 1167 (1977).

<sup>3</sup>E. Abrahams, P. W. Anderson, D. C. Licciardello, and T. V. Ramakrishnan, Phys. Rev. Lett. **42**, 673 (1979).



- <sup>4</sup>P. W. Anderson, E. Abrahams, and T. V. Ramakrishnan, *Phys. Rev. Lett.* **43**, 718 (1979).
- <sup>5</sup>L. P. Gorkov, A. I. Larkin, and D. E. Khmel'nitskii, *Pis'ma Zh. Eksp. Teor. Fiz.* **30**, 248 (1979) [*JETP Lett.* **30**, 248 (1979)].
- <sup>6</sup>B. L. Altshuler, D. E. Khmel'nitskii, A. I. Larkin, and P. A. Lee, *Phys. Rev. B* **22**, 5142 (1980).
- <sup>7</sup>S. Hikami, A. I. Larkin, and Y. Nagaoka, *Prog. Theor. Phys.* **63**, 707 (1980).
- <sup>8</sup>B. L. Altshuler, A. G. Aronov, and B. V. Spivak, *Pis'ma Zh. Eksp. Teor. Fiz.* **34**, 285 (1981) [*JETP Lett.* **33**, 94 (1981)].
- <sup>9</sup>For reviews of weak localization, see G. Bergmann, *Phys. Rep.* **107**, 1 (1984); or S. Chakravarty and A. Schmid, *ibid.* **140**, 193 (1986).
- <sup>10</sup>D. Yu Sharvin and Yu. V. Sharvin, *Pis'ma Zh. Eksp. Teor. Fiz.* **34**, 285 (1981) [*JETP Lett.* **34**, 272 (1981)].
- <sup>11</sup>R. A. Webb, S. Washburn, C. P. Umbach, and R. B. Laibowitz, *Phys. Rev. Lett.* **54**, 2696 (1985).
- <sup>12</sup>For reviews of Aharonov Bohm experiments in rings and cylinders, see S. Washburn and R. A. Webb, *Adv. Phys.* **35**, 375 (1986); and A. G. Aronov and Yu. V. Sharvin, *Rev. Mod. Phys.* **59**, 755 (1987).
- <sup>13</sup>C. P. Umbach, S. Washburn, R. B. Laibowitz, and R. A. Webb, *Phys. Rev. B* **30**, 4048 (1984); J. C. Licini, D. J. Bishop, M. A. Kastner, and J. Melngailis, *Phys. Rev. Lett.* **55**, 2987 (1985).
- <sup>14</sup>R. G. Wheeler, K. K. Choi, and R. Wisniewski, *Surf. Sci.* **142**, 19 (1984); W. J. Skocpol, L. D. Jackel, R. E. Howard, H. G. Craighead, L. A. Fetter, P. M. Mankiewich, P. Grabbe, and D. M. Tenant, *ibid.* **142**, 14 (1984).
- <sup>15</sup>B. L. Altshuler, *Pis'ma Zh. Eksp. Teor. Fiz.* **41**, 530 (1985) [*JETP Lett.* **41**, 648 (1985)].
- <sup>16</sup>A. D. Stone, *Phys. Rev. Lett.* **54**, 2692 (1985); P. A. Lee and A. D. Stone, *ibid.* **55**, 1622 (1985); P. A. Lee, A. D. Stone, and H. Fukuyama, *Phys. Rev. B* **35**, 1039 (1987).
- <sup>17</sup>B. L. Altshuler, A. G. Aronov, and D. E. Khmel'nitskii, *J. Phys. C* **15**, 7367 (1982).
- <sup>18</sup>W. Eiler, *J. Low Temp. Phys.* **56**, 481 (1984).
- <sup>19</sup>H. Fukuyama and E. Abrahams, *Phys. Rev. B* **27**, 5976 (1983).
- <sup>20</sup>J. M. B. Lopes dos Santos, *Phys. Rev. B* **28**, 1189 (1983).
- <sup>21</sup>A. Schmid, *Z. Phys.* **271**, 251 (1974).
- <sup>22</sup>J. J. Lin and N. Giordano, *Phys. Rev. B* **33**, 1519 (1986).
- <sup>23</sup>S. Wind, M. J. Rooks, V. Chandrasekhar, and D. E. Prober, *Phys. Rev. Lett.* **57**, 633 (1986).
- <sup>24</sup>A review of many weak localization experiments in 2D films is given by Bergmann in Ref. 9.
- <sup>25</sup>A. Stern, Y. Aharonov, and Y. Imry, *Phys. Rev. A* **41**, 3436 (1990).
- <sup>26</sup>V. Chandrasekhar, P. Santhanam, and D. Prober, *Phys. Rev. B* **44**, 11 203 (1991). These authors suggest on p. 11 219 that perhaps  $L_{\phi}^{\text{UCF}} > L_{\phi}^{\text{WL}}$ . Our experiments show the opposite result.
- <sup>27</sup>P. McConville and N. O. Birge, *Phys. Rev. B* **47**, 16 667 (1993).
- <sup>28</sup>Ya. M. Blanter, *Phys. Rev. B* **54**, 12 807 (1996).
- <sup>29</sup>P. Mohanty, E. M. Q. Jariwala, and R. A. Webb, *Phys. Rev. Lett.* **78**, 3366 (1997).
- <sup>30</sup>B. L. Altshuler, M. E. Gershenson, and I. L. Aleiner, *Physica E Spectra* **3**, 58 (1998).
- <sup>31</sup>J. H. Scofield, *Rev. Sci. Instrum.* **58**, 985 (1987).
- <sup>32</sup>The presence of spin-flip scattering is difficult to distinguish from an apparent saturation of  $L_{\phi}$  versus temperature in the temperature range of this experiment. At lower temperatures, dilute magnetic impurities give rise to the Kondo effect, and a logarithmic temperature dependence of  $L_{\phi}$ . See, for example, Ref. 29.
- <sup>33</sup>E. L. Altshuler, B. L. Altshuler, and A. G. Aronov, *Solid State Commun.* **54**, 617 (1985).
- <sup>34</sup>W. Eiler, *Solid State Commun.* **56**, 917 (1985).
- <sup>35</sup>For a review of  $1/f$  noise, see M. B. Weissman, *Rev. Mod. Phys.* **60**, 537 (1988).
- <sup>36</sup>P. Dutta and P. M. Horn, *Rev. Mod. Phys.* **53**, 497 (1981).
- <sup>37</sup>N. O. Birge, B. Golding, and W. H. Haemmerle, *Phys. Rev. Lett.* **62**, 195 (1989); *Phys. Rev. B* **42**, 2735 (1990).
- <sup>38</sup>J. S. Moon, N. O. Birge, and B. Golding, *Phys. Rev. B* **53**, R4193 (1996); **56**, 15 124 (1997).
- <sup>39</sup>D. E. Beutler, T. L. Meisenheimer, and N. Giordano, *Phys. Rev. Lett.* **58**, 1240 (1987); T. L. Meisenheimer and N. Giordano, *Phys. Rev. B* **39**, 9929 (1989).
- <sup>40</sup>G. A. Garfunkel, G. B. Alers, M. B. Weissman, J. M. Mochel, and D. J. VanHarlingen, *Phys. Rev. Lett.* **60**, 2773 (1988); G. B. Alers, M. B. Weissman, R. A. Averbach, and H. Shyu, *Phys. Rev. B* **40**, 900 (1989).
- <sup>41</sup>B. L. Al'tshuler and B. Z. Spivak, *Pis'ma Zh. Eksp. Teor. Fiz.* **42**, 363 (1985) [*JETP Lett.* **42**, 447 (1985)].
- <sup>42</sup>S. Feng, P. A. Lee, and A. D. Stone, *Phys. Rev. Lett.* **56**, 1960 (1986); **56**, 2772(E) (1986).
- <sup>43</sup>B. L. Altshuler and B. I. Shklovskii, *Zh. Eksp. Teor. Fiz.* **91**, 220 (1986) [*Sov. Phys. JETP* **64**, 127 (1986)].
- <sup>44</sup>A. D. Stone, *Phys. Rev. B* **39**, 10 736 (1989).
- <sup>45</sup>S. Feng, *Phys. Rev. B* **39**, 8722 (1989).
- <sup>46</sup>O. Millo, S. J. Klepper, M. W. Keller, D. E. Prober, S. Xiong, A. D. Stone, and R. N. Sacks, *Phys. Rev. Lett.* **65**, 1494 (1990).
- <sup>47</sup>V. Chandrasekhar, P. Santhanam, and D. E. Prober, *Phys. Rev. B* **42**, 6823 (1990).
- <sup>48</sup>J. Pelz and J. Clarke, *Phys. Rev. B* **36**, 4479 (1987).
- <sup>49</sup>A unified approach to UCF noise and local interference noise has been presented by S. Herschfield, *Phys. Rev. B* **37**, 8557 (1988).
- <sup>50</sup>H. Fukuyama, *J. Phys. Soc. Jpn.* **53**, 3299 (1984).
- <sup>51</sup>P. M. Echternach, M. E. Gershenson, H. M. Bozler, A. L. Bogdanov, and B. Nilsson, *Phys. Rev. B* **48**, 11 516 (1993).
- <sup>52</sup>P. J. McConville, Ph.D. thesis, Michigan State University, 1995.